

Dirac Phase interferometer in a plasmonic waveguide

V. Savinov*

Optoelectronics Research Centre & Centre for Photonic Metamaterials, University of Southampton SO17 1BJ, UK

N. I. Zheludev

Optoelectronics Research Centre & Centre for Photonic Metamaterials, University of Southampton SO17 1BJ, UK and
Centre for Disruptive Photonic Technologies, TPI,
Nanyang Technological University, Singapore 637371, Singapore

By viewing plasmon waves in metallic waveguides as propagating electric and magnetic dipoles we show that according to laws of quantum mechanics they will acquire additional phase when propagating through space with static magnetic field. The new effect is physically different from conventional magneto-plasmonic phenomena and is sufficiently strong to observe it under routinely accessible experimental conditions.

The Aharonov-Bohm (AB) effect is both one of the most celebrated and vigorously debated effects in quantum physics [1, 2]. It is a quantum mechanical topological phenomenon in which phase of an electrically charged particle is affected by the presence of magnetic field, even if the particle is confined to a region in which the field is zero. The modern interpretation of this phenomenon is that the dynamics of the electrons are affected by the magnetic vector potential rather than by the magnetic field.

The Aharonov-Bohm effect arises as a result of Dirac's magnetic phase factor [3–5], the extra phase gained by the electrons propagating in the electromagnetic potential. There are other similar effects that also arise due to Dirac's phase factor. In particular, in the Aharonov-Casher (AC) effect the phase is gained by the particle with permanent magnetic dipole due to propagation in electric field [6], whilst in the He-McKellar-Wilkens (HMW) effect [7, 8], the phase is gained by the particles with permanent electric dipole that propagate in magnetic field.

All three effects described above have now been experimentally observed. The Aharonov-Bohm effect was demonstrated by Tonomura [9]. In his experiment electrons were made to pass through and around a toroidal solenoid and then their interference pattern was recorded. The Aharonov-Casher effect was tested with neutron [10] and atomic interferometry [11], and was also observed in solid-state systems [12, 13] as well as in Josephson junctions [14, 15]. The He-McKellar-Wilkens effect was only confirmed recently by interfering trains of polarized lithium atoms [16–19].

The focus of our paper will be the He-McKellar-Wilkens effect illustrated in Fig. 1. Consider a train of traveling particles with permanent electric (**p**) and magnetic dipole (**m**) moments. The train is passed through a particle interferometer where it is split in two branches which are routed along different paths, and are then joined back together into a single train. If the interferometer is placed into magnetic field (**B**), the phase of the

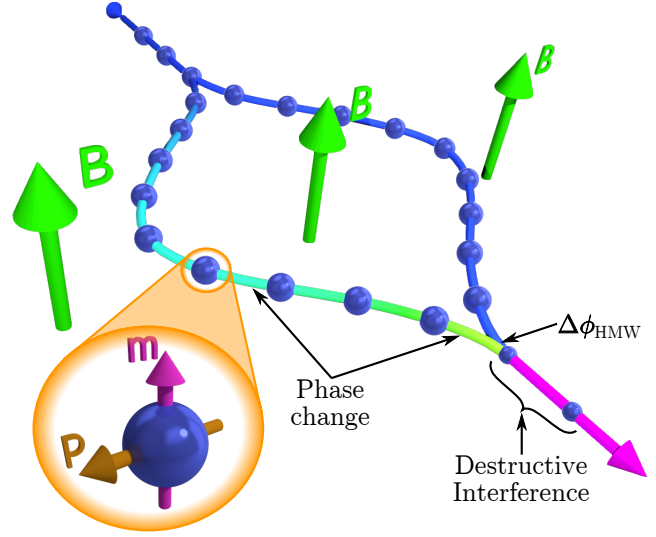


Figure 1: **Illustration of the He-McKellar-Wilkens effect.** Neutral particles with permanent electric (**p**) and magnetic (**m**) dipoles are passed through an interferometer in the presence of externally applied magnetic field (**B**). Propagation of particles leads to change in their phase. If the magnetic field is different at the two arms of the interferometer, or if the lengths of the two arms are different, the phase difference ($\Delta\phi_{HMW}$) can be detected through interference of the particles.

particles in the two branches of the train will be shifted by an amount that will depend on the magnetic field strength. This will lead to magnetically tunable particle interference at the output of the interferometer.

In this paper we will show that the He-McKellar-Wilkens effect can be observed with surface plasmon-polaritons propagating in static magnetic field. Surface plasmon-polaritons are coupled oscillations of light and electron plasma in metals. These propagating coupled oscillations can be described as quantum-mechanical particles propagating along the waveguide trajectory. The correspondence between the wave and particle pictures is established by assuming that particles carry electric and

magnetic dipole moments corresponding to the classical polarization (\mathbf{P}) and magnetization (\mathbf{M}) of the guided wave. We will now show that the phase gain by plasmon-polaritons due to He-McKellar-Wilkens effect will be observable under routinely accessible experimental conditions in a plasmonic waveguide.

The Lagrangian for a neutral particle with permanent electric (\mathbf{p}) and magnetic (\mathbf{m}) dipole moments moving at velocity \mathbf{v} through electromagnetic field is [6, 8, 17, 20] :

$$L = L_{kin} + L_{self} + \\ + \mathbf{E} \cdot \left(\mathbf{p} + \frac{1}{c^2} \mathbf{v} \times \mathbf{m} \right) + \mathbf{B} \cdot \left(\mathbf{m} - \mathbf{v} \times \mathbf{p} \right) \quad (1)$$

Where \mathbf{E} and \mathbf{B} denote the electric and magnetic fields, respectively. Above, L_{kin} denotes the kinetic part of the Lagrangian and L_{self} denotes the Lagrangian due to interaction of the dipoles with their fields. These two terms will be of no interest to us in what is to follow, as the effect in question is related to the last two terms in the Lagrangian.

A quantum mechanical particle described by the Lagrangian from Eq. (1) will gain phase as a result of propagation. The path-specific expression for the phase gain ($\Delta\phi$) due to transition from point \mathbf{r}_a at time t_a to point \mathbf{r}_b at time t_b can be written in terms of action (S) divided by reduced Planck constant (\hbar):

$$\Delta\phi = S[\mathbf{r}]/\hbar = \frac{1}{\hbar} \int_{t_a}^{t_b} dt L = \\ = \Delta\phi_{kin} + \Delta\phi_{self} + \\ + \frac{1}{\hbar} \int_{t_a}^{t_b} dt (\mathbf{p} \cdot \mathbf{E} + \mathbf{m} \cdot \mathbf{B}) + \\ + \frac{1}{\hbar} \int_{\mathbf{r}_a}^{\mathbf{r}_b} d\mathbf{r} \cdot \left(\frac{1}{c^2} \mathbf{m} \times \mathbf{E} - \mathbf{p} \times \mathbf{B} \right) \quad (2)$$

In Eq. (2) the fourth term includes phase gained due to increased or reduced energy of the electric and magnetic dipoles in the electromagnetic field. The last term of Eq. (2) differs significantly from the preceding terms in being expressed through an integral along a path rather than a temporal integral. It is relevant to both the He-McKellar-Wilkens and the Aharonov-Casher effects. For the rest of this paper we will concentrate on the He-McKellar-Wilkens effect, we therefore set $\mathbf{E} = \mathbf{0}$. The phase gained by the particle as a direct result of propagation in the magnetic field, without the additional terms, is then given by:

$$\Delta\phi_{HMW} = \Delta\phi - (\Delta\phi_{kin} + \Delta\phi_{self}) = \\ = \frac{1}{\hbar} \int_{t_a}^{t_b} dt \mathbf{m} \cdot \mathbf{B} - \frac{1}{\hbar} \int_{\mathbf{r}_a}^{\mathbf{r}_b} d\mathbf{r} \cdot (\mathbf{p} \times \mathbf{B}) \quad (3)$$

The He-McKellar-Wilkens effect is significantly more difficult to observe than the Aharonov-Bohm and

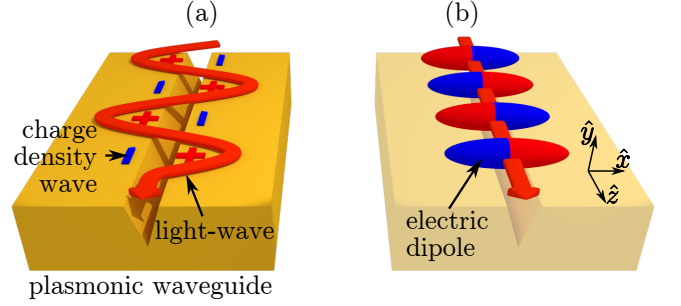


Figure 2: **Viewing plasmonic waveguide with guided light-wave as a stream of propagating dipoles.** (a) A sketch of a light-wave propagating along a plasmonic waveguide. The propagating radiation is accompanied by induced co-propagating charge density wave (shown with '+' and '-' signs). (b) The charge density wave propagating along the waveguide (as shown in (a)) can be viewed as a stream of anti-aligned dipoles propagating along the waveguide. For simplicity only the electric dipoles are shown in the sketch, in reality however there are also co-propagating magnetic dipoles aligned along the y-axis.

Aharonov-Casher phenomena. Indeed, due to lack of elementary particles with electric dipole, the recent observations of this effect have been obtained by *inducing* a polarization in otherwise non-polarized charge-current distribution of the lithium atoms [16–19]. We argue that it should be possible to observe the He-McKellar-Wilkens effect in the traveling waves of *induced polarization* in metals, i.e. surface plasmon-polaritons. For simplicity we shall consider plasmon waves in a V-groove plasmonic waveguide, as is shown in Fig. 2. Since in a linear waveguide the induced polarization scales with amplitude of the guided mode, one should expect the He-McKellar-Wilkens phase shift in the waveguide to be a function of the power of the guided mode.

For the following analysis we will adopt a specific waveguide geometry with opening angle of 25° and depth of $3 \mu\text{m}$ (see Fig. 3). We will also assume that the waveguide is made of gold (dielectric constant taken from Ref. [21]) and that the ambient environment is vacuum (or air). Furthermore we shall assume that the free-space wavelength of the light propagating along the waveguide is $\lambda_0 = 1.31 \mu\text{m}$ and that the power carried by the waveguide is $\mathcal{P} = 1 \mu\text{W}$. These assumptions are in no way mandatory for observation of the effect, instead they represent a set of conditions that can be easily accessed in the experiment.

We proceed by breaking up the continuous traveling charge (ρ) and current (\mathbf{J}) density waves into individual half-periods, and finding the electric (\mathbf{p}) and magnetic

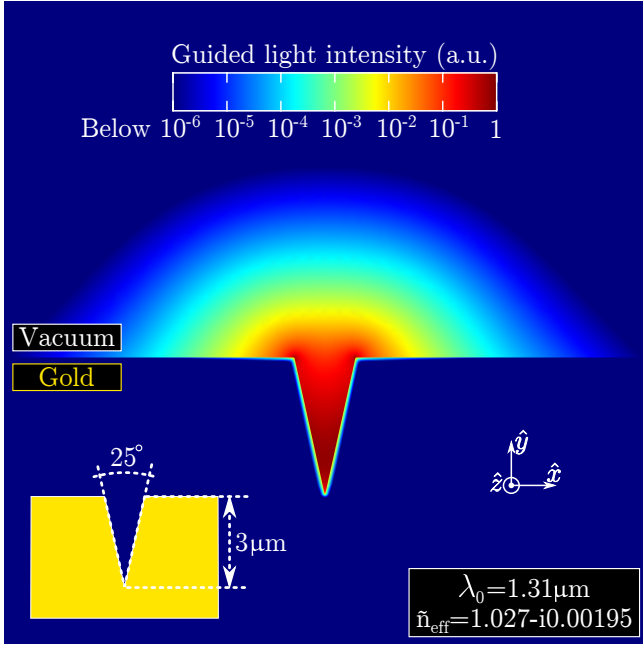


Figure 3: **Simulation of the guided mode in the exemplary waveguide.** The main plot shows the log-scale colourmap of the intensity of guided radiation in the waveguide. The waveguide is made of gold and is operating in free-space environment. The free-space wavelength of the guided mode is $\lambda_0 = 1.31 \mu\text{m}$. The inset on the bottom left-hand side shows the details of the waveguide geometry.

(m) dipole moments of each half-period using [22]:

$$\mathbf{p} = \int d^3r \rho \mathbf{r} = \frac{1}{i\omega} \int d^3r \mathbf{J}$$

$$\mathbf{m} = \frac{1}{2} \int d^3r [\mathbf{r} \times \mathbf{J}]$$

where the integral is taken over the volume occupied by a single half-period.

Numerical simulation of the mode guided by the waveguide, shown in Fig. 3, allows to determine the effective refractive index of the mode $\tilde{n}_{eff} = 1.027 - i0.00195$ as well as the distribution of the electric field ($\mathbf{E}_{mode}(x, y)$) in the xy-plane, the plane perpendicular to the direction of mode propagation (along the z-axis). Ignoring the losses in the waveguide ($n_{eff} \equiv \Re(\tilde{n}_{eff})$) we can write the full distribution of the electric field as $\mathbf{E}(\mathbf{r}) = \mathbf{E}_{mode}(x, y) \times \exp\left(-i\frac{2\pi}{\lambda_0} n_{eff} z\right)$ and the full current density distribution as $\mathbf{J} = i\omega \epsilon_0 \left(\tilde{\epsilon}_r^{(Au)} - 1\right) \mathbf{E}$, where ϵ_0 is the free-space permittivity and $\tilde{\epsilon}_r^{(Au)} = -79.1 - i7.02$ is the dielectric constant of gold at $\lambda_0 = 1.31 \mu\text{m}$ [21]. Consequently, the expressions for the single-half-period

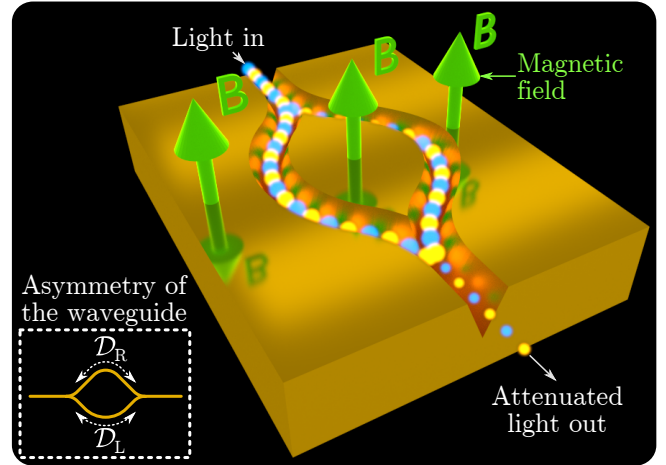


Figure 4: **Detection of He-McKellar-Wilkens effect with a plasmonic V-groove interferometer.** The guided light-wave and the co-propagating stream of dipoles (see Fig. 2) is split and recombined in an interferometer. As is shown in the schematic on the bottom-left inset, the interferometer is asymmetric with the lengths of the left (D_L) and the right (D_R) arms being different ($\Delta D = D_R - D_L \neq 0$). Applying magnetic field (\mathbf{B}) perpendicular to interferometer plane will, through the He-McKellar-Wilkens effect, induce an additional phase difference between surface plasmon-polaritons propagating along the left and the right arms. The phase difference will be proportional to the applied magnetic field, and the transmission of the interferometer will be a function of the applied magnetic field.

dipoles become:

$$\mathbf{p} = \epsilon_0 \left(\tilde{\epsilon}_r^{(Au)} - 1\right) \int_{-\frac{\lambda_0}{4n_{eff}}}^{\frac{\lambda_0}{4n_{eff}}} dz \int dx dy \mathbf{E}(\mathbf{r}) \quad (4)$$

$$\mathbf{m} = \frac{i\omega \epsilon_0 \left(\tilde{\epsilon}_r^{(Au)} - 1\right)}{2} \int_{-\frac{\lambda_0}{4n_{eff}}}^{\frac{\lambda_0}{4n_{eff}}} dz \int dx dy [\mathbf{r} \times \mathbf{E}(\mathbf{r})] \quad (5)$$

Numerically evaluating the integrals in Eq. (4,5) we find, up to a complex phase, $\mathbf{p} = (9.8 \times 10^{-27} \text{ C.m}) \hat{\mathbf{x}}$ and $\mathbf{m} = (4.1 \times 10^{-17} \text{ J/T}) \hat{\mathbf{y}}$. One should note that by the nature of the guided mode in the plasmonic waveguide the two dipoles are perpendicular to each other ($\mathbf{p} \perp \mathbf{m}$), and to the direction of propagation, at all times ($\mathbf{p}, \mathbf{m} \perp \mathbf{v}$, where \mathbf{v} is the velocity of the guided mode).

The He-McKellar-Wilkens phase shift of the guided plasmonic mode can be detected in a plasmonic interferometer as is shown in Fig. 4. Using the fact that the magnetic dipole, electric dipole and the velocity are always mutually perpendicular ($\mathbf{p} \perp \mathbf{m} \perp \mathbf{v}$) the expres-

sions in Eq. (3) can be simplified to:

$$\begin{aligned}\Delta\phi_{HMW} &= \frac{B}{\hbar} (\mathcal{T}m - \mathcal{D}p) \\ &= \frac{B\mathcal{D}}{\hbar} \left(\frac{n_{eff}}{c} m - p \right)\end{aligned}\quad (6)$$

Above we have assumed the configuration in which the applied magnetic field is perpendicular to waveguide plane (as in Fig. 4), and is therefore parallel to the magnetic dipole ($\mathbf{B} \parallel \mathbf{m}$). The duration and the length of propagation are denoted with \mathcal{T} and \mathcal{D} respectively. From Eq. (6) it follows that if the interferometer is symmetric the surface plasmon-polaritons propagating along the different arms will gain the same phase due to He-McKellar-Wilkens effect. However, an asymmetry of the interferometer ($\Delta\mathcal{D} \neq 0$ in Fig. 4) can give rise to the additional difference in phase of the surface plasmon-polaritons traveling along the two interferometer arms:

$$\Delta\phi_{HMW} = \frac{B \cdot \Delta\mathcal{D}}{\hbar} \cdot \left(\frac{n_{eff}}{c} m - p \right) \quad (7)$$

For $\Delta\mathcal{D} = 200$ nm and $B = 10$ mT one finds:

$$\Delta\phi_{HMW} = \underbrace{2.6 \text{ rad}}_m - \underbrace{0.19 \text{ rad}}_p$$

The phase difference $\Delta\phi_{HMW}$ scales linearly with magnetic field (B), with length difference of the interferometer arms ($\Delta\mathcal{D}$), and with magnitudes of the two dipole moments (m and p). The dipole magnitudes, in turn, scale as the square-root of the power (\mathcal{P}) guided by the plasmonic interferometer. One can therefore quantify the He-McKellar-Wilkens effect in a plasmonic interferometer in terms of a dimensional constant:

$$\Lambda_{HMW} = \frac{\Delta\phi_{HMW}}{\Delta\mathcal{D} \cdot B \cdot \sqrt{\mathcal{P}}} \approx 1200 \text{ rad}/(\text{nm.T.}\sqrt{\text{W}})$$

It is important to note that in plasmonic He-McKellar-Wilkens effect the transmission of the interferometer depends both on the applied magnetic field and on the power of the guided mode, consequently this effect cannot be ascribed to Faraday effect or to any other linear, i.e. power-independent, magneto-optical phenomena. It should also be noted that, in contrast to conventional magneto-optical effects, in the plasmonic He-McKellar-Wilkens effect the mechanism of modulation of interferometer transmission is not linked to material used to implement the waveguide, instead the modulation arises as an intrinsic property of the charge carriers that give rise to the plasmon waves. Finally we address the scaling of the observable effect with optical power. To remain within the quasi-particle model, we shall assume that the asymmetry of the interferometer is small ($\cos(\Delta\phi_{HMW}) \approx 1 - \frac{1}{2}\Delta\phi_{HMW}^2$), and thus the observable interferometer disbalance due to He-McKellar-Wilkens effect will scale linearly with guided power.

In conclusion, we have proposed and analyzed a plasmonic version of the He-McKellar-Wilkens effect. We have shown that this effect can be observed under routinely accessible strengths of magnetic field and power of electromagnetic radiation, using a plasmonic waveguide interferometer. The proposed effect will allow the development of a new generation of compact magneto-optical modulators and may be used for tuning active plasmonic devices such as spaser [23–25].

This study was supported by the Engineering and Physical Sciences Research Council (grant EP/G060363/1), the Royal Society, and the Singapore Ministry of Education [Grant MOE2011-T3-1-005]. Authors gratefully acknowledge enlightening discussions with Prof. M. Stockman from Georgia State University (USA).

* Electronic address: vs1106@orc.soton.ac.uk

- [1] W. Ehrenberg and R. E. Siday, “The refractive index in electron optics and the principles of dynamics,” *Proc. Phys. Soc. B*, vol. 62, no. 1, pp. 8–21, 1949.
- [2] Y. Aharonov and D. Bohm, “Significance of electromagnetic potentials in the quantum theory,” *Phys. Rev.*, vol. 115, p. 485, 1959.
- [3] P. A. M. Dirac, “Quantized singularities in the electromagnetic field,” *Proc. Roy. Soc. Lond. A*, vol. 133, pp. 60–72, 1931.
- [4] M. V. Berry, “Exact Aharonov-Bohm wavefunction obtained by applying Dirac’s magnetic phase factor,” *Eur. J. Phys.*, vol. 1, pp. 240–244, 1980.
- [5] ——, “Asymptotics of the many-whirls representation for Aharonov-Bohm scattering,” *J. Phys. A: Math. Theor.*, vol. 43, p. 354002, 2010.
- [6] Y. Aharonov and A. Casher, “Topological quantum effects for neutral particles,” *Phys. Rev. Lett.*, vol. 53, pp. 319–321, 1984.
- [7] X.-G. He and B. H. J. McKellar, “Topological phase due to electric dipole moment and magnetic monopole interaction,” *Phys. Rev. A*, vol. 47, no. 4, pp. 3424–3425, 1993.
- [8] M. Wilkens, “Quantum phase of a moving dipole,” *Phys. Rev. Lett.*, vol. 72, no. 1, pp. 5–8, 1994.
- [9] A. Tonomura, N. Osakabe, T. Matsuda, T. Kawasaki, J. Endo, S. Yano and H. Yamada, “Evidence for Aharonov-Bohm effect with magnetic field completely shielded from electron wave,” *Phys. Rev. Lett.*, vol. 56, no. 8, pp. 792–795, 1986.
- [10] A. Cimmino, G. I. Opat, and A. G. Klein, H. Kaiser, S. A. Werner, M. Arif, and R. Clothier, “Observation of the topological Aharonov-Casher phase shift by neutron interferometry,” *Phys. Rev. Lett.*, vol. 63, no. 4, pp. 380–383, 1989.
- [11] K. Sangster, E. A. Hinds, S. M. Harnett and E. Riis, “Measurement of the Aharonov-Casher phase in an atomic system,” *Phys. Rev. Lett.*, vol. 71, no. 22, pp. 3641–3844, 1993.
- [12] M. König *et al.*, “Direct observation of the Aharonov-Casher phase,” *Phys. Rev. Lett.*, vol. 96, p. 076804, 2006.
- [13] F. Qu *et al.*, “Aharonov-Casher effect in Bi_2Se_3 square-

ring interferometers,” *Phys. Rev. Lett.*, vol. 107, p. 016802, 2011.

[14] W. J. Elion, J. J. Wachters, L. L. Sohn, and J. E. Mooij, “Observation of the Aharonov-Casher effect for vortices in Josephson-Junction arrays,” *Phys. Rev. Lett.*, vol. 71, no. 14, pp. 2311–2314, 1993.

[15] I. M. Pop *et al.*, “Experimental demonstration of Aharonov-Casher interference in a Josephson junction circuit,” *Phys. Rev. B*, vol. 85, p. 094503, 2012.

[16] S. Lepoutre, A. Gauguet, G. Tréneau, M. Büchner, and J. Vigué, “He-McKellar-Wilkens topological phase in atom interferometry,” *Phys. Rev. Lett.*, vol. 109, p. 120404, 2012.

[17] J. Gillot, S. Lepoutre, A. Gauguet, M. Büchner, and J. Vigué, “Measurement of the He-McKellar-Wilkens topological phase by atom interferometry and test of its independence with atom velocity,” *Phys. Rev. Lett.*, vol. 111, p. 030401, 2013.

[18] S. Lepoutre, A. Gauguet, M. Büchner, and J. Vigué, “Test of the He-McKellar-Wilkens topological phase by atom interferometry. I. Theoretical discussion,” *Phys. Rev. A*, vol. 88, p. 043627, 2013.

[19] ———, “Test of the He-McKellar-Wilkens topological phase by atom interferometry. II. The experiment and its results,” *Phys. Rev. A*, vol. 88, p. 043628, 2013.

[20] J. Anandan, “Classical and quantum Interaction of the dipole,” *Phys. Rev. Lett.*, vol. 85, no. 7, pp. 1354–1357, 2000.

[21] P. B. Johnson and R. W. Christy, “Optical constants of the noble metals,” *Phys. Rev. B*, vol. 6, p. 4370, 1972.

[22] J. D. Jackson, *Classical Electrodynamics*. Wiley, New York ed. 3, 1999.

[23] D. J. Bergman and M. I. Stockman, “Surface plasmon amplification by stimulated emission of radiation: quantum generation of coherent surface plasmons in nanosystems,” *Phys. Rev. Lett.*, vol. 90, p. 027402, 2003.

[24] M. I. Stockman, “Spasers explained,” *Nature Photon.*, vol. 2, pp. 327–329, 2008.

[25] N. I. Zheludev, S. L. Prosvirnin, N. Papasimakis and V. A. Fedotov, “Lasing spaser,” *Nature Photon.*, vol. 2, pp. 351–354, 2008.